Wet compression model for entropy production minimization

Gudjonsdottir, Vilborg; Infante Ferreira, Carlos; Goethals, A.

DOI
10.1016/j.applthermaleng.2018.12.065
Publication date
2019
Document Version
Final published version
Published in
Applied Thermal Engineering

Applied Thermal Engineering 149 (2019) 439–447

Contents lists available at ScienceDirect

Applied Thermal Engineering

journal homepage: www.elsevier.com/locate/apthermeng

Research Paper

Wet compression model for entropy production minimization

V. Gudjonsdottir[a,*], C.A. Infante Ferreira[a], A. Goethals[b]

[a] Process and Energy Laboratory, Delft University of Technology, Leeghwaterstraat 39, 2628 CB, Delft, the Netherlands
[b] Atlas Copco Airpower N. V., Compressor Technique, Boomsesteenweg 957, P.O. Box 101, 2610 Wilrijk, Belgium

HIGHLIGHTS

- The compressor efficiency makes CRHP performance condition dependent.
- The efficiency is largely dependent on the vapor quality and NH_3 concentration.
- At lower vapor qualities liquid limits leakages and entropy production.
- The locations of the ports are important to minimize losses.
- For identical clearances the sealing line losses are the largest losses.

ARTICLE INFO

Keywords:
Twin-screw compressor
Wet compression
Ammonia-water
Entropy production generation

ABSTRACT

Compression-resorption heat pumps (CRHP) utilizing wet compression are a very promising option to upgrade waste heat from industry. CRHPs have the potential to have higher coefficient of performance (COP) than the traditionally used vapour-compression heat pumps (VCHP). However, commercial solutions utilizing wet compression are not available yet. Also, wet compression is a feasible option only if the efficiency of the compressor is sufficiently high, 0.7 or higher, as identified by several authors. In this study, we develop and validate a model of a twin screw compressor that is suitable for wet compression. The model is adapted to calculate the entropy production generation in order to identify where the major irreversibilities are located in the compressor. The effects of clearance size, rotational speed, ammonia concentrations, compressor inlet vapor quality as well as under- and over compression are analysed. The results show that the clearance size and the rotational speed have the largest effects on the entropy production. Additionally, increased ammonia concentration and decreased vapor quality lead to decreased losses. The results indicate that it should be feasible to reach the targeted performance if the clearances size is limited to 50 μm, the rotational speed maintained above 10,000 rpm, the ammonia concentration kept in the range of 30–40 wt.%, and the inlet vapor quality in the range 0.5–0.7.

1. Introduction

The industry is responsible for approximately quarter of the final energy consumption in Europe [7]. Heat pumps have the potential to drastically reduce energy requirements in the industry and in that way reduce emissions [13]. Van de Bor et al. [26] compared different heat pump technologies and for industrial applications where there is a temperature glide of the heat source and/or sink compression-resorption heat pumps (CRHP) utilizing wet compression can achieve higher coefficient of performance (COP) than alternative technologies. Van de Bor et al. however assumed an isentropic efficiency of 70% for the compressor. If this limit is not reached there might be no advantage of wet compression compared to the traditionally used vapor compression heat pump (VCHP) as pointed out by several authors [10,27]. In wet compression the process is entirely in the two phase region instead of in the vapor region. Zaytsev [27] identified a twin screw compressor as the most suitable type of compressor for wet compression since it is tolerant for liquid carry over and can have a rather high efficiency. He performed experiments with a twin screw compressor utilizing wet compression with additional liquid injection, however, he reached only efficiencies of around 6–7%. Infante Ferreira et al. [9] performed further experiments with a prototype twin screw compressor, and they reached isentropic efficiencies of around 35%. Since then quite a number of experiments have been performed with twin screw compressors with liquid injection were high efficiencies have been achieved, around or higher than 70% [4,20]. In these cases liquid is

* Corresponding author.
E-mail address: v.gudjonsdottir@tudelft.nl (V. Gudjonsdottir).

https://doi.org/10.1016/j.applthermaleng.2018.12.065
Received 13 June 2018; Received in revised form 29 October 2018; Accepted 12 December 2018
Available online 13 December 2018

Nomenclature

A	area, m^2
a,b	constants for Blasius equation, –
C	dynamic bearing load, N
d	diameter, m
h	specific enthalpy, $J\,kg^{-1}$
L	length, m
$\dot{m}$	mass flow, $kg\,s^{-1}$
m	mass, kg
m_1	number of male lobes, –
n	rotation speed, rpm
p	pressure, Pa
$\dot{Q}$	heat transfer rate, W
Q	heat, J
s	specific entropy, $J\,kg^{-1}\,K^{-1}$
T	temperature, K
v	specific volume, $m^3\,kg^{-1}$
V	volume, m^3
$\dot{V}$	volume flow rate, $m^3\,s^{-1}$
w	flow velocity, $m\,s^{-1}$
W	work, J
$\dot{W}$	power, W
x	ammonia mass concentration, $kg\,kg^{-1}$

Greek

ρ	density, $kg\,m^{-3}$
η	efficiency, –
μ	dynamic viscosity, Pa s/coefficient of friction, –
$\dot{\sigma}$	entropy production rate, $W\,K^{-1}$
φ	male rotor turning angle
ζ	flow coefficient
ω	angular rotation speed, s^{-1}

Sub- and superscripts

b	bearing
d	discharge
$down$	downstream
h	hydraulic
id	ideal
in	inlet
is	isentropic
max	maximum
$mech$	mechanical
out	outlet
$real$	real
s	suction/seal
$seal$	labyrinth seal
th	theoretical
$total$	total
up	upstream
vol	volumetric

injected during vapor compression, however, few studies have been performed with ammonia-water. Tian et al. [25] recently performed experiments with ammonia-water mixture in an ammonia refinery, therefore with high concentrations of ammonia. They investigated two sets of compressors, in the first one liquid was injected to a superheated ammonia stream, 98 wt.% NH_3, and it reached an isentropic efficiency of around 75 wt.%. In the second one liquid was injected to a saturated ammonia stream at higher temperature and pressure and an efficiency of 64% was reached. For CRHP the ideal situation is to compress within the two-phase region at all times. Therefore, it is necessary to further study the influence of compression within the two-phase region and to investigate if isentropic efficiencies above 70% are still a feasible option.

Different modeling approaches have been used in the literature to simulate the performance of twin screw compressors. For the thermodynamic performance most of them are 1 D cavity models with different level of accuracy like the ones used by Cao et al. [4], Chamoun et al. [5], Jianfeng et al. [11], Seshaiah et al. [19], and Tian et al. [24]. In recent years computation fluid dynamics (CFD) models of twin screw compressors have gained increased attention and a comparison was recently made by Kennedy et al. [12] for oil free dry compression. In their study the thermodynamic cavity model gave more accurate results and for wet compression the CFD model will be even more challenging. However, as pointed out by these authors the CFD model gives an idea of the complex internal flow phenomena which can be useful for the design of twin screw compressors though difficult to validate. In this study a 1 D cavity model based on the work of Zaytsev [27] is developed, validated and modified to include entropy production generation. This model is chosen since it should give sufficient accuracy to evaluate the performance of wet compression in a twin screw compressor. Entropy production generation allows identification of the locations of irreversibilities in the system. In this study the effects of the clearance size, ammonia concentration, rotational speed, vapor quality at the inlet of the compressor, and location of the discharge port are investigated. The results give an idea of the optimal operating conditions of such a compressor in a CRHP operating with ammonia-water as a working fluid.

2. The screw compressor model

The screw compressor model is based on a model described by Zaytsev [27]. The model is divided in a geometry model and a thermodynamic model. The geometry model was developed by Zaytsev [27] and is based on the meshing line between the two rotors. For a detailed description of the geometry model see Zaytsev and Infante Ferreira [28]. Table 1 gives some geometrical data of the studied compressor. Additionally, some details of the adopted compressor geometry are illustrated in Fig. 1 to clarify the determination of the port sizes and leakage path areas.

The model is not described here further, however, it does give essential information for further thermodynamic calculations; the cavity volume, the suction area, the discharge area and the leakage areas. The thermodynamic model is described in the following section.

2.1. Thermodynamic model

The thermodynamic model is a homogenous model based on mass and energy conservations [27]. This model is assumed to be of sufficient

Table 1
Rotor main geometrical characteristics [27].

Rotor length, mm	172.5
Distance between the axis, mm	77.1
Number of male rotor lobes	5
Number of female rotor lobes	6
Wrap angle of the male rotor, °	314
Diameter of the male rotor, mm	104.9
Diameter of the female rotor, mm	80
Estimated average clearance, μm	200*

* The value used by Zaytsev [27] during his validation.

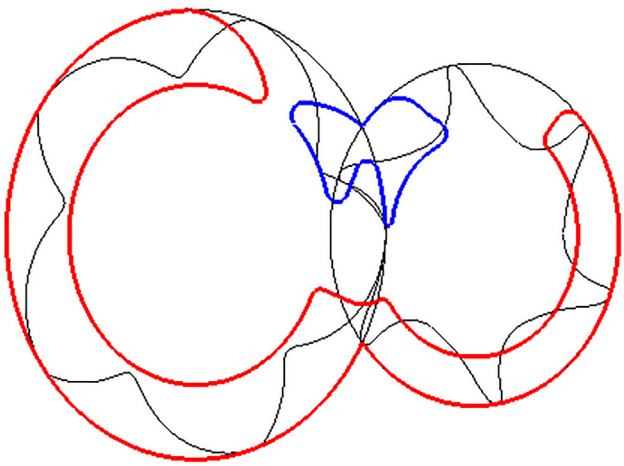

Fig. 1. Geometry of the rotors and shape of the radial suction port in red (there is also an axial suction port) and discharge port in blue.

detail to give reliable results for wet compression. The main reasons are that in contrast to liquid injected process, in wet compression the liquid and vapor are already at equilibrium at the inlet of the compressor. Additionally, Stosic et al. [22] concluded that for oil injected process the oil follows closely the gas temperature during the compression process in a twin screw compressor for droplet sizes less than 0.5 mm. Therefore, by spraying the liquid into the vapor flow at the compressor inlet, close to homogenous conditions should be attained. The mass conservation can be defined in the following way:

$$\frac{dp}{d\varphi} = \frac{1}{\left(\frac{\partial v}{\partial p}\right)_{T,x}}\left[\frac{v}{m}\left(\sum_{k=1}^{n}\left(\frac{dm_{out}}{d\varphi}\right)_k - \sum_{k=1}^{n}\left(\frac{dm_{in}}{d\varphi}\right)_k\right) + \frac{1}{m}\frac{dV}{d\varphi} - \left(\frac{\partial v}{\partial T}\right)_{P,x}\frac{dT}{d\varphi}\right] \tag{1}$$

And the energy conservation can be written in the following form:

$$\frac{dT}{d\varphi} = \frac{T\left(\frac{\partial v}{\partial T}\right)_{P,x}\left[\frac{v}{m}\left(\sum_{k=1}^{n}\left(\frac{dm_{out}}{d\varphi}\right)_k - \sum_{k=1}^{l}\left(\frac{dm_{in}}{d\varphi}\right)_k\right) + \frac{1}{m}\frac{dV}{d\varphi}\right]}{\left(\frac{\partial v}{\partial p}\right)_{T,x}\left(\frac{\partial h}{dT}\right)_{p,x} + T\left(\frac{\partial v}{\partial T}\right)^2_{P,x}} + \frac{\frac{\partial Q}{d\varphi} + \sum_{k=1}^{l}(h_{in,k} - h)\left(\frac{dm_{in}}{d\varphi}\right)_k}{m\left(\frac{\partial h}{dT}\right)_{p,x} + \frac{mT}{\left(\frac{\partial v}{\partial p}\right)_{T,x}}\left(\frac{\partial v}{\partial T}\right)^2_{P,x}} \tag{2}$$

The mass flow rate, depending on the male rotation angle, through both the suction and discharge ports as well as due to the leakages is calculated with the continuity equation:

$$\frac{dm}{d\varphi} = \frac{\zeta\rho A w}{\omega} \tag{3}$$

where ζ is the empirical flow coefficient, A the leakage area, ρ density of the flow, ω the angular speed of the male rotor and the flow velocity, w, is determined by the converging nozzle model:

$$w = \sqrt{2\int_{P_{down}}^{P_{up}} v dp} \tag{4}$$

With the maximum limit being the local speed of sound

$$w_{\max} = v\sqrt{-\left(\frac{\partial p}{\partial v}\right)_{is}} \tag{5}$$

The overall mass flow rate can then be calculated as

$$\dot{m} = m_1\frac{n}{60}\int\frac{dm}{d\varphi}d\varphi \tag{6}$$

The model takes into account the main leakage paths in a screw compressor, which are;

1. Through the contact line between the two rotors.
2. Through the sealing line between the tip of the rotors and the housing.
3. Through the cusp blowholes at compression side with high pressure.
4. Through the compression-start blowholes at the suction side.
5. Through the discharge end clearance.

The isentropic efficiency of the compressor is defined as:

$$\eta_{is} = \frac{\dot{m}(h_{id,d} - h_s)}{\dot{W}} \tag{7}$$

where the power input, $\dot{W}$, is defined as

$$\dot{W} = \dot{m}\int V dp \tag{8}$$

The volumetric efficiency is defined as the ratio of the real and theoretical volumetric displacement:

$$\eta_{vol} = \frac{\dot{V}_{real}}{\dot{V}_{th}} \tag{9}$$

where $\dot{V}_{real} = v_s\int\frac{dm}{d\varphi}d\varphi$ and $\dot{V}_{th}$ is the maximum cavity volume.

2.2. Mechanical losses

In the literature it is common to assume a fixed mechanical efficiency [1,25,5], normally in the range 0.9 to 0.95. However, as experiments from Arjeneh et al. [2] show the mechanical losses do increase with increased rotational speed. In this work one of the goals is to estimate the effects of the rotational speed and therefore assuming a fixed value for the mechanical efficiency would not result in the most realistic results. It is assumed that the main contributors to the mechanical losses are:

- Bearings
- Seals
- Gears

It is assumed that there are four radial and two axial bearings and the losses are estimated with the following equation [21]

$$\dot{W}_b = 5.25\cdot10^{-6}\mu C d_b n \tag{10}$$

where μ is the coefficient of friction and C is the dynamic bearing load, both given by the manufacturer.

To estimate the sealing losses an equation from Parker Hannifin Corporation [16] for elastomer shaft seals is used. As noted by them this should only be used as an estimate and the real value will depend on many factors like the seal design, shaft texture, pressures and time in service.

$$\dot{W}_s = 7.45\cdot10^{-7}d_s n^{4/3} \tag{11}$$

They indicate that the power input needed for a dry running seal will be two to three times the value above. In the calculations it is assumed that the power input will therefore be three times the estimated value.

Further it is assumed that the losses caused by gear meshing and synchronization are 4% [3]. As pointed out by Zaytsev [27] it is difficult to estimate to what degree these losses will affect the process medium itself. Similar to Zaytsev [27] it is assumed that only the sealing losses will have effects on the process medium at the beginning of the suction process, as heat input ($\frac{\partial Q}{d\varphi}$ in Eq. (2)). The total isentropic efficiency of the system is then defined as the product of the isentropic

efficiency and the mechanical efficiency. It should be noted that motor losses are not taken into account.

$$\eta_{is,total} = \eta_{is}\eta_{mech} \tag{12}$$

2.3. Entropy production

The model takes into account the rate of entropy production generation which for systems operating in steady state can be defined as [14]:

$$\dot{\sigma} = \sum_k \dot{m}_k s_k - \sum_j \dot{m}_j s_j - \sum_i \frac{\dot{Q}_i}{T_i} \tag{13}$$

The entropy production is then calculated as a function of the male rotation angle to observe the entropy production throughout the compression process. In each control volume all inlet and outlet mass flows are considered and their respective properties, e.g. if there is a leakage flow from the following cavity the entropy is a function of the conditions of that cavity. The heat losses to the environment are assumed negligible, except for the sealing losses influencing the process medium at the start of the suction process.

$$\frac{d\sigma}{d\varphi} = \sum_{k=1}^{n}\left(\frac{dm_{out}}{d\varphi}s_{out}\right)_k - \sum_{k=1}^{n}\left(\frac{dm_{in}}{d\varphi}s_{in}\right)_k \tag{14}$$

The model is implemented in Matlab. The conservation equations are solved with the Heun method. The thermodynamic properties of the ammonia-water mixture needed for the calculations, including the entropy, are calculated with the computational method developed by Rattner and Garimella [18]. To include the leakage calculations first the model is run without any leakages. Then the model is run including the leakages until the solution converges to acceptable tolerances, which was chosen as 0.1% change in isentropic efficiency. Compared to the model of Zaytsev [27], the model is now implemented in Matlab, a new thermodynamic property method is used and the mechanical loss estimation has been modified. Therefore, a validation is necessary and is implemented in the following section.

3. Model validation

A new twin screw compressor prototype is being built that will be used in the near future to test wet compression. Since the prototype is not ready, experimental data from Zaytsev [27] are used for validation purposes, the geometrical characteristics are listed in Table 1 and the experimental results and their accuracy are listed in Table 2. Although the efficiencies attained during this experiment were quite low, this experiment has been selected since only Zaytsev's work reports oil-free ammonia-water compression in a twin-screw compressor with sufficient detail to be used for validation purposes. The low efficiencies were caused by mainly the use of a labyrinth seal which created a large leakage flow from discharge to inlet nozzle and the large manufacturing tolerances. These processes can be added to the model for validation purposes. Both the compressor used for validation purposes and the compressor studied in this manuscript have bearing being oil lubricated outside the process side of the compressor. In the compressor used for validation purposes labyrinth and lip seals were used to separate the oil lubricated and the oil-free process sides of the compressor. In the compressor discussed in this manuscript only lip seals separate the process side from the oil lubricated side. Liquid ammonia-water was used as the lubricant in the compressor used for validation purposes. In the present study synchronization gears are used to prevent contact between the two rotors so that no lubrication is required. The main differences between the prototype used by Zaytsev and the current one under study are that Zaytsev [27] used not only wet compression but also liquid injection of ammonia-water. In the new prototype no liquid is injected, the two-phase working fluid (ammonia-water) is compressed directly.

Both liquid injection, added power input caused by friction, and the leakage caused by the labyrinth seal are implemented in the validation, however, they are not applicable for the new prototype and are therefore not implemented in the analysis in the following chapter. Nannan [15] analyzed the leakage flow through the labyrinth seal. The method that gave the best results was the one developed by Eser and Kazakia [6]. The one used by Zaytsev [27], the Blasius equation was, however, not far off and is easier to implement and is therefore used:

$$\dot{m} = \rho A\left(\frac{2d_h\Delta p}{\rho a L_{seal}}\right)^{\frac{1}{2+b}}\left(\frac{\rho d_h}{\mu}\right)^{\frac{-b}{2+b}} \tag{15}$$

During the experiments of Zaytsev [27] liquid was injected between angles 60 to 384°. When liquid is added the ammonia concentration changes throughout the control volume which can be expressed with the following equation:

$$\frac{dx}{d\varphi} = \frac{1}{m}\left[\left(\sum_{k=1}^{n} x_{in,k}\left(\frac{dm_{in}}{d\varphi}\right)_k - x\sum_{k=1}^{n}\left(\frac{dm_{in}}{d\varphi}\right)_k\right)\right] \tag{16}$$

Also additional terms need to be added to the conservation equations, Eqs. (1) and (2). And they can be written in the following form:

$$\frac{dp}{d\varphi} = \frac{1}{\left(\frac{\partial v}{\partial p}\right)_{T,x}}\left[\frac{v}{m}\left(\sum_{k=1}^{n}\left(\frac{dm_{out}}{d\varphi}\right)_k - \sum_{k=1}^{n}\left(\frac{dm_{in}}{d\varphi}\right)_k\right) + \frac{1}{m}\frac{dV}{d\varphi} - \left(\frac{\partial v}{\partial T}\right)_{P,x}\frac{dT}{d\varphi} - \left(\frac{\partial v}{\partial x}\right)_{p,T}\frac{dx}{d\varphi}\right] \tag{17}$$

And the energy conservation can be written in the following form:

$$\frac{dT}{d\varphi} = \frac{T\left(\frac{\partial v}{\partial T}\right)_{P,x}\left[\frac{v}{m}\left(\sum_{k=1}^{n}\left(\frac{dm_{out}}{d\varphi}\right)_k - \sum_{k=1}^{l}\left(\frac{dm_{in}}{d\varphi}\right)_k\right) + \frac{1}{m}\frac{dV}{d\varphi} - \left(\frac{\partial v}{\partial x}\right)_{p,T}\frac{dx}{d\varphi}\right]}{\left(\frac{\partial v}{\partial p}\right)_{T,x}\left(\frac{\partial h}{dT}\right)_{p,x} + T\left(\frac{\partial v}{\partial T}\right)^2_{P,x}} + \frac{\frac{\partial Q}{d\varphi} + \sum_{k=1}^{l}(h_{in,k} - h)\left(\frac{dm_{in}}{d\varphi}\right)_k - m\left(\frac{\partial h}{\partial x}\right)_{p,T}\frac{dx}{d\varphi}}{m\left(\frac{\partial h}{dT}\right)_{p,x} + \frac{mT}{\left(\frac{\partial v}{\partial p}\right)_{T,x}}\left(\frac{\partial v}{\partial T}\right)^2_{P,x}} \tag{18}$$

Comparison of the experimental data, the current model and the model developed by Zaytsev is shown in a *p-V* diagram in Fig. 2, and comparison of the calculated and measured efficiencies are listed in Table 3. The estimated uncertainty of the isentropic and volumetric efficiency of the compressor from Zaytsev are 18% and 12%, respectively [27]. As can be seen the current model can estimate the overall performance of the compressor within these error boundaries. Since it is similar to the model of Zaytsev it similarly underestimates the pressure during compression and slightly overestimates the pressure at the discharge side. It should be noted that the exact clearances of the compressor are not really known since they were not measured accurately

Table 2
Experimental results from Zaytsev [27].

Suction pressure, bar(a)	3.70 ± 0.08 bar
Discharge pressure, bar(a)	9.08 ± 0.13 bar
Injection pressure, bar(a)	4.19 ± 0.13 bar
Suction temperature, °C	62.8 ± 0.5 °C
Discharge temperature, °C	97.6 ± 0.8 °C
Injection temperature, °C	64 ± 0.5 °C
Ammonia concentration suction, kg kg^{-1}	0.359 ± 6%
Injection concentration suction, kg kg^{-1}	0.284 ± 10%
Injection flow rate, kg s^{-1}	0.14 ± 1%
Shaft speed, rpm	3500 ± 7 rpm

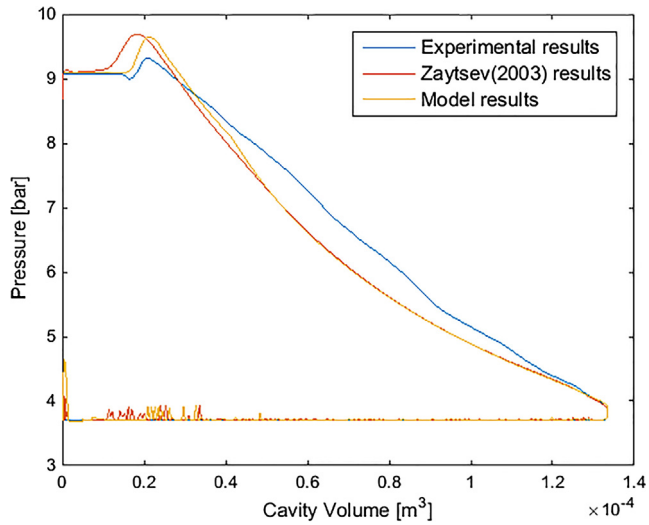

Fig. 2. Comparison of experimental data from Zaytsev [27], his model and the current model results.

Table 3
Comparison of efficiencies, discharge temperature and discharge flow rate between the experimental data from Zaytsev [27], his model and the current model.

	Measured	Zaytsev	Current model
Isentropic efficiency, %	5.2	5.6	5.9
Volumetric efficiency, %	7.4	7.2	7.4
Discharge temperature, °C	97.6	98.2	98.4
Discharge flow rate, kg/s	0.078	0.070	0.077

by Zaytsev. He mentions in his work that the main reason for the extremely low efficiencies was caused by large clearances. They were both kept large to ensure safe operation taken into account thermal expansion during operation and also they were increased because of rotor wear. It should also be noted that the flow coefficient used for the leakage flow is kept the same as adopted by Zaytsev or 1.2. The flow coefficients used for the suction and discharge flows are 0.8 and 0.6, respectively. Several authors have investigated flow coefficients including Fujiwara and Osada [8], and Prins and Infante Ferreira [17]. It is clear from those studies that the flow coefficients have quite a large range (in the aforementioned studies values from 0.4 to 1.22) and will depend on the specific geometry, working fluid and operating conditions. Since Zaytsev had similar conditions his coefficients have been used. It should be pointed out that the location of the discharge port was moved by two rotational degrees to better match the experimental data.

4. Analysis and discussion

In the following subsections the effects of the main operational parameters are further studied. Another field of study that is not discussed here is the optimization of the geometry of a twin screw compressor as has been done by e.g. Stosic et al. [23]. As mentioned in the previous section, experiments with a new screw compressor prototype are planned in the near future. Unfortunately the detailed geometry is not available therefore the same geometry as defined by Zaytsev is used for the analysis. One uncertainty of the new prototype are the clearances. The two rotors are kept apart by timing gears and additionally the clearances can change during operation due to thermal expansion. However, the rotational speed will be significantly larger. The compressor in practice should be able to operate from around 10,000 until 32,000 rpm which is considerably higher than the 3500 rpm from

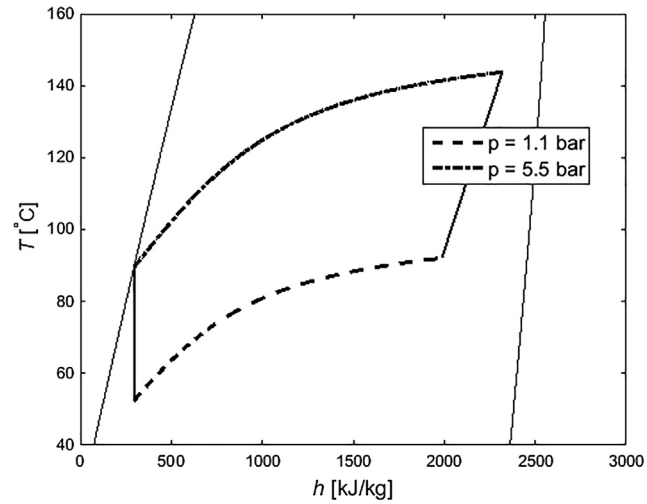

Fig. 3. *T-h* diagram of a CRHP for 30 wt.% NH_3.

Zaytsevs experiments. Therefore, the effects of clearance size as well as different rotational speeds are investigated in the following sections.

For the prototype there is a minimum pressure limit of around 1.1 bar. This limit is because of the shaft seals that are used. If the pressure is lower there is a danger of oil leaking into the compressor and limiting its performance. In the analysis the discharge pressure is set to 5.5 bar. An example of the CRHP system for 30 wt.% NH_3 is shown in Fig. 3. The temperature range could be suitable to many potential industrial applications. As mentioned by Chamoun et al. [5] large amount of waste heat at 80–90 °C is available in various industrial sectors where higher temperatures are needed, typically around 120–130 °C. Additionally, the production of steam where at the same time there is a heat source with a temperature glide is an attractive option for CRHP. The location of the discharge port is modified for each case so that it gives results close to perfect compression. The effects of under and over- compression are additionally analysed in the last subsection of this section. Ammonia concentrations in the range from 20 to 40 wt.% NH_3 are investigated since they are normally of interest for CRHP where the heat source and or heat sink have a large temperature glide. The analysed cases are listed in Table 4.

4.1. Clearance size

In this part the results from cases 1–4 from Table 4 are discussed. In Fig. 4 the entropy production for each leakage path are shown as a function of the male rotor angle for average clearance of 10 μm and 100 μm. In Fig. 5 the *p-V* diagrams of the same cases are shown. The results from case 2 are approximately in between the other two cases. In Table 5 the entropy production of leakages, the overall entropy

Table 4
Different operating cases that are investigated.

Nr.	Average ammonia concentration, kg/kg	Clearance, μm	rpm	Inlet vapor quality
1	30	10	10,000	0.6
2	30	50	10,000	0.6
3	30	100	10,000	0.6
4	30	200	10,000	0.6
5	30	50	3500	0.6
6	30	50	5000	0.6
7	30	50	20,000	0.6
8	30	50	30,000	0.6
9	20	50	10,000	0.6
10	40	50	10,000	0.6
11	30	50	10,000	0.5
12	30	50	10,000	0.7

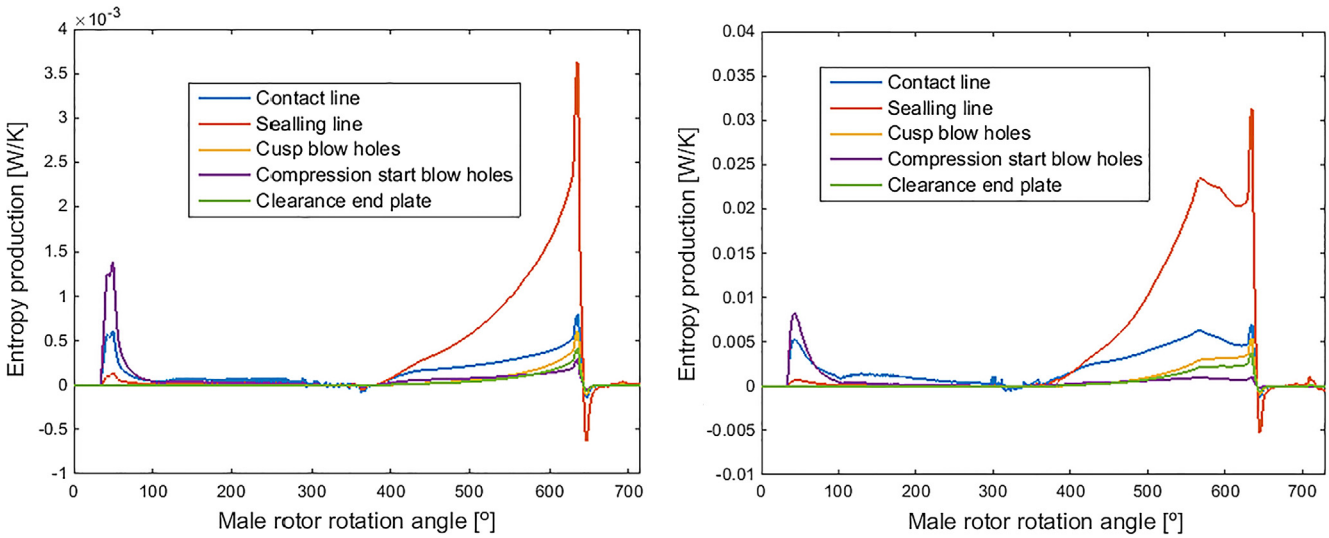

Fig. 4. $\dot{\sigma}$ for each leakage path in the compressor, 10 µm (left) and 100 µm (right).

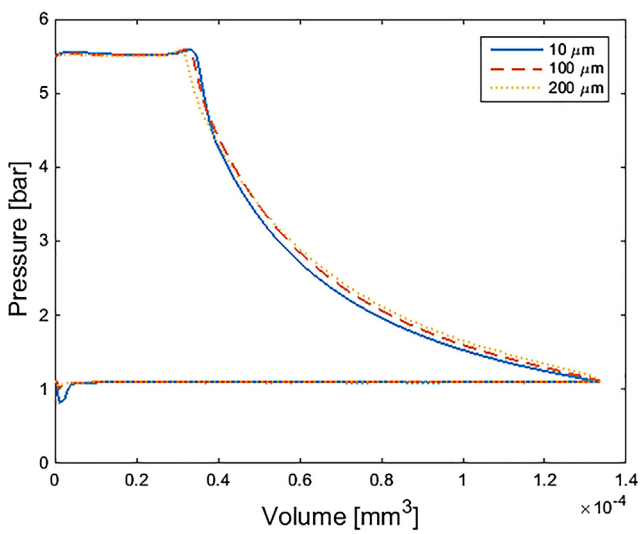

Fig. 5. *p-V* diagram for 10 µm (blue solid line), 100 µm (red dashed line) and for 200 µm (yellow dotted line).

production as well as the isentropic efficiencies are listed for the cases. As expected with larger clearances the efficiency decreases and the entropy production increases. In both cases a small cause of entropy production is at the start of the suction process. The suction process is approximately until male rotation angle of 400° where the compression process starts until the discharge port is opened around an angle of 650°. At the start of the suction process there is already a small volume available in the compressor before the suction cavity opens. When the clearances are small this causes a slight pressure and temperature drop. With larger clearances the leakages flows are large enough to maintain the pressure (see Fig. 5). This shows the importance of a well located suction port. In both cases the largest losses are caused by leakages through the sealing line during the compression process. However, there is a large shift to the left (see Fig. 4) during the compression process with increased clearance since larger amount leaks back. This can also be seen from the shift in pressure during the compression process in the *p-V* diagram in Fig. 5. The second largest contributor is leakage through the contact line of the two rotors. It should be noted that the contribution of the leakages are closely related to the clearance of each leakage path. Here an average clearance is assumed. The clearances can be different for each leakage path, along the leakage path and also vary throughout the compression process, for example, for the sealing line due to thermal expansion. Using locally measured clearances can modify these results. In Table 5 the main results are listed.

4.2. Rotational speed

In Table 6 the isentropic efficiency as well as the overall entropy production for cases 2, 5–8 are listed. Chamoun et al. [5] investigated water vapor compression with injected liquid and similarly the efficiency increases with increased rotational speed. Similar trend can be seen here up to a certain point. This difference can be explained by the increase in mechanical losses. As mentioned earlier, experiments conducted by Arjeneh et al. [2] showed that the mechanical losses increase with the rotational speed. When the rotational speed increases also the flow of working fluid through the compressor increases. So in this case a larger entropy production (which follows from the larger flow) is not necessarily negative since there is also a larger displacement of working fluid. Here the isentropic efficiency gives a better indication of which operating condition is more advantageous. Nevertheless also here the entropy production allows for identification of the major sources of irreversibility in the compressor and remains relevant.

4.3. Ammonia concentration

Depending on each industrial application a specific ammonia

Table 5
Isentropic efficiencies, entropy production of the leakages and overall entropy production of cases 1–4.

Nr.	Clearance, µm	η_{is}	$\eta_{is,\ total}$	$\dot{W}$, kW	Entropy production of leakages in, W/K	Entropy production of leakages out, W/K	Overall entropy production, W/K
1	10	0.78	0.70	21.8	0.4	0.2	10.9
2	50	0.71	0.63	22.0	2.5	1.1	13.6
3	100	0.63	0.57	22.4	5.8	2.8	16.6
4	200	0.45	0.41	22.5	11.8	6.2	18.3

Table 6
Isentropic efficiencies and overall entropy production of cases 2, 5–8.

Nr.	rpm	η_{is}	$\eta_{is,\ total}$	$\dot{W}$, kW	Entropy production of leakages in, W/K	Entropy production of leakages out, W/K	Overall entropy production, W/K
5	3500	0.57	0.45	7.9	2.3	3.4	7.0
6	5000	0.65	0.54	11.1	8.8	8.4	8.2
2	10,000	0.71	0.63	22.0	2.5	1.1	13.6
7	20,000	0.75	0.70	44.0	2.1	1.0	21.6
8	30,000	0.73	0.69	67.2	3.0	1.9	26.9

Table 7
Isentropic efficiencies and overall entropy production of cases 2, 9 and 10.

Nr.	Average ammonia concentration, kg/kg	η_{is}	$\eta_{is,\ total}$	$\dot{W}$, kW	Entropy production of leakages in, W/K	Entropy production of leakages out, W/K	Overall entropy production, W/K
9	20	0.68	0.60	22.1	2.4	1.0	13.9
2	30	0.71	0.63	22.0	2.5	1.1	13.6
10	40	0.72	0.64	21.9	2.1	1.1	12.6

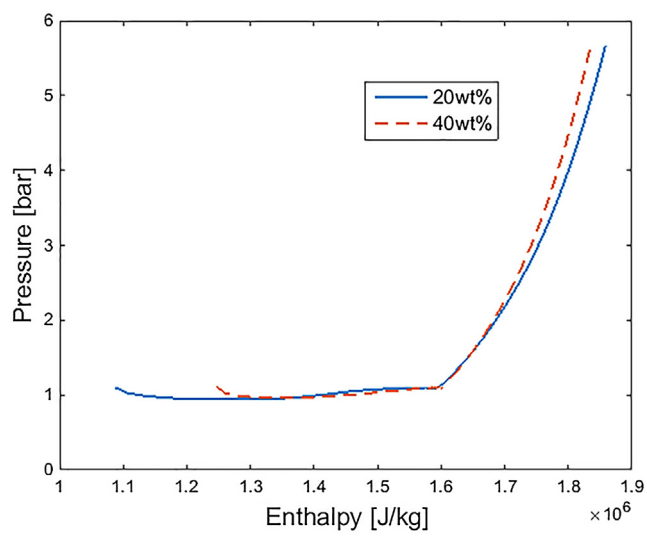

Fig. 6. *p-h* diagram, 20 wt.% (blue solid line) and 40 wt.% (red dashed line).

concentration will give the optimum results for a CRHP. As mentioned earlier, for large number of industrial application cases the optimum ammonia concentration is in the range of 20 to 40 wt.% ammonia. In Table 7 the entropy production of leakages, the overall entropy production as well as the isentropic efficiencies are listed for the cases with different ammonia concentration. Even though the isentropic efficiency increases with increasing ammonia concentration as well as the overall entropy production decreases the effects of the leakages are similar for all 3 cases. In Fig. 6 the difference between 20 wt.% ammonia versus 40 wt.% ammonia is displayed in a *p-h* diagram. The different mixtures have of course quite different properties and with increasing ammonia concentration for a similar process it is clear from the figure that less work is needed for the same compression ratio. It should be noted that different concentrations will lead to different temperature levels. Therefore, this does not mean that for every application it is optimal to operate at higher concentration of ammonia. However, this might cause a slight shift in the optimal ammonia concentration.

4.4. Vapor quality

For CRHP the optimum outlet vapor quality is saturated vapor (quality = 1.0) if it is assumed that the compressor has a fixed isentropic efficiency [26]. In practice this might be difficult to reach since the temperature increases drastically if the working fluid goes into the superheated region. If the working fluid starts to superheat the temperature rises quickly and the compressor could be damaged because of thermal expansion. Reversed the compressor will also be damaged with excessive liquid level. Higher inlet quality than 0.7 is not possible in this case since the outlet quality at the end of the compression process is close to being saturated vapor. For this reason only the inlet quality range 0.5 to 0.7 will be investigated.

In Table 8 the main results are listed. Cao et al. [4] performed experiments with varied gas volume fraction for an oil flooded twin screw compressor. Even though entirely a different mixture they obtained similar results, that is with a lower gas volume fraction the efficiency increased since the liquid partially blocks the leakage paths. In Fig. 7 the entropy production is displayed for case 2 and 12. The differences are small, however, the difference can be most clearly seen in the decreased losses caused by the contact line during the suction period (until a male rotation angle of approximately 400°). The entropy production caused by the leakages decreases at lower vapor qualities while the overall entropy production increases. The increase in the overall entropy production can be explained by a slight increase in the overall mass flow at lower inlet qualities. From these results it is clear that it is not satisfactory to use a fixed isentropic efficiency for evaluation of the performance of an CRHP.

4.5. Under and over-compression

In Table 9 the main results from shifting the discharge port by 5°to the left and right for case number 2 (from Table 4) are listed. The results are additionally shown in a *p-V* diagram in Fig. 8. From under and over compressing the efficiency decreases slightly while the entropy production stays more or less the same. This results from slight differences

Table 8
Isentropic efficiencies and overall entropy production of cases 2, 11 and 12.

Nr.	Inlet vapor quality	η_{is}	$\eta_{is,\ total}$	$\dot{W}$, kW	Entropy production of leakages in, W/K	Entropy production of leakages out, W/K	Overall entropy production, W/K
11	0.5	0.72	0.64	21.6	2.0	1.0	14.1
2	0.6	0.71	0.63	22.0	2.5	1.1	13.6
12	0.7	0.70	0.62	22.4	3.4	0.0	13.1

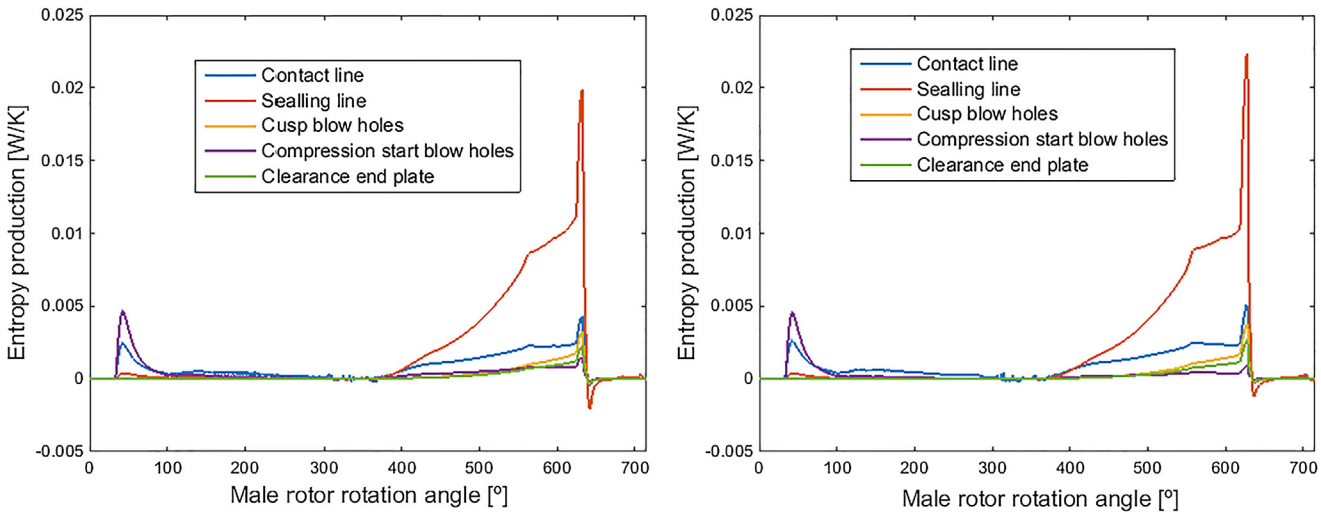

Fig. 7. $\dot{\sigma}$ for each leakage path in the compressor, 0.6 inlet vapor quality (left) and 0.7 inlet vapor quality (right).

Table 9
Isentropic efficiencies and overall entropy production of cases 2 with under and over compression.

Nr.	Under or over compression	η_{is}	$\eta_{is,\ total}$	$\dot{W}$, kW	Entropy production of leakages in, W/K	Entropy production of leakages out, W/K	Overall entropy production, W/K
2	Under	0.70	0.62	22.4	2.3	1.1	13.7
2	–	0.71	0.63	22.0	2.5	1.1	13.6
2	Over	0.69	0.62	22.4	2.4	1.2	13.6

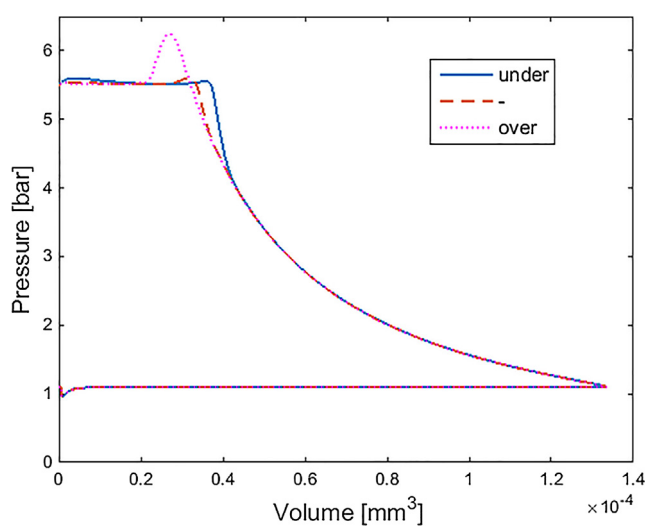

Fig. 8. *p-V* diagram for under compression (blue solid line), close to perfect compression (red dashed line) and for over compression (magenta dotted line).

in the overall mass flow. A small degree of under or over compressing should therefore not have a large impact on the overall performance. Of course with a larger deviation the performance will continue to decrease and therefore should be avoided at all cost.

5. Conclusions

This paper has introduced the use of local entropy generation to identify the causes of thermodynamic irreversibilities in twin-screw compressors operating oil-free with two-phase ammonia-water as working fluid:

- For identical clearance sizes, the sealing line losses lead to the largest thermodynamic losses of the twin-screw compressor;
- An increase of the clearance size from 10 to 100 μm leads to 10 times larger sealing line losses;
- Since the working fluid flow increases with the rotational speed of the compressor the overall entropy production also increases while the energetic performance may increase. In this case a larger entropy production is not necessarily disadvantageous;
- The effect of ammonia-water concentration on the entropy production losses is limited, higher concentration leads to a small decrease of the entropy production;
- A lower quality at the compressor inlet indicates that more liquid is available for limiting the leakages and so the entropy production;
- Small deviations of the position of the discharge port lead to small under- or over-compression with small changes of the entropy production.

The paper has additionally investigated, for a specific geometry, if a twin-screw compressor is capable of attaining isentropic efficiencies higher than 0.7 so that it will deliver competitive performance results when implemented in wet compression resorption heat pumps. The study has indicated that:

- Clearance sizes should be limited to 50 μm;
- Rotational speed should be maintained above 10000 rpm;
- Ammonia-water concentration should preferably be maintained in the range 30 to 40 wt.%;
- The vapor quality at the inlet of the compressor should be maintained in the range 0.5 to 0.7;
- Under and over-compression should be avoided at all costs.

In general can be concluded that the compressor efficiency will strongly depend on the operating conditions so that, when predicted the efficiency of wet compression resorption heat pumps, the specific efficiency needs to be taken into account.

Acknowledgments

This is an ISPT (Institute for Sustainable Process Technology) project.

References

[1] I.M. Arbon, The design and application of rotary twin-shaft compressors in the oil and gas industry, Mech. Eng. Publ. (1994).
[2] M. Arjeneh, A. Kovacevic, S. Rane, M. Manorils, N. Stosic, Numerical and experimental investigation of pressure losses of a twin screw compressor, IOP Conf. Ser.: Mater. Sci. Eng. 90 (2015) 012006, , https://doi.org/10.1088/1757-899X/90/1/012006.
[3] Beardmore, R. (2013). Gear efficiency. Retrieved from http://www.roymech.co.uk/Useful_Tables/Drive/Gear_Efficiency.html.
[4] F. Cao, T. Gao, S. Li, Z. Xing, P. Shu, Experimental analysis of pressure distribution in a twin screw compressor for multiphase duties, Exp. Therm Fluid Sci. 35 (1) (2011) 219–225, https://doi.org/10.1016/j.expthermflusci.2010.09.004.
[5] M. Chamoun, R. Rulliere, P. Haberschill, J. Peureux, Modelica-based modeling and simulation of a twin screw compressor for heat pump applications, Appl. Therm. Eng. 58 (1–2) (2013) 479–489, https://doi.org/10.1016/j.applthermaleng.2013.04.020.
[6] D. Eser, J.Y. Kazakia, Air flow in cavities of labyrinth seals, Int. J. Eng. Sci. 30 (1995) 2309–2326.
[7] European Council. 2030 Climate and energy policy framework, 2014.
[8] M. Fujiwara, Y. Osada, Performance analysis of an oil-injected screw compressor and its application, Int. J. Refrig. 18 (1995) 220–227.
[9] C.A. Infante Ferreira, C. Zamfirescu, D. Zaytsev, Twin screw oil-free wet compressor for compression–absorption cycle, Int. J. Refrig. 29 (2006) 556–565.
[10] L.C.M. Itard, Wet compression versus dry compression in heat pumps working with pure refrigerants or non-azetropic mixtures, Int. J. Refrig. 18 (1995) 495–504.
[11] L. Jianfeng, W. Huagen, W. Bingming, X. Ziwen, S. Pengcheng, Research on the performance of water-injection twin screw compressor, Appl. Therm. Eng. 29 (16) (2009) 3401–3408, https://doi.org/10.1016/j.applthermaleng.2009.05.018.
[12] S. Kennedy, M. Wilson, S. Rane, Combined numerical and analytical analysis of an oil-free twin screw compressor numerical analysis of an oil-free twin screw compressor using 3D CFD and 1D multi-chamber thermodynamic model, IOP Conf. Ser.: Mater. Sci. Eng. 232 (2017), https://doi.org/10.1088/1757-899X/232/1/012080.
[13] A.A. Kiss, C.A. Infante-Ferreira, Heat pumps in chemical process industry, CRC-Press, (Taylor & Francis Group), US, 2016.
[14] J.M. Moran, H.N. Shapiro, Fundamentals of engineering thermodynamics, sixth ed., John Wiley and Sons, 2010.
[15] Nannan, N.R., Analysis of the leakage flow through the labyrinth seal of the ammonia-water two-phase screw compressor. Master thesis, Delft University of Technology, 2004.
[16] Parker Hannifin Corporation. Rotary Seals: Rotary Seals Design Guide. Catalog EPS 5350/USA, 2017.
[17] J. Prins, C.A. Infante Ferreira, Quasi one-dimensional steady-state models for gas leakage Part II: Improvement of the viscous modeling, in: International Compressor Enginering Conference, Purdue University, Indiana, 1998.
[18] A.S. Rattner, S. Garimella, Fast, stable computation of thermodynamic properties of ammonia-water mixtures, Int. J. Refrig. 62 (2015) 39–59.
[19] N. Seshaiah, S.K. Ghosh, R.K. Sahoo, S.K. Sarangi, Mathematical modeling of the working cycle of oil injected rotary twin screw compressor, Appl. Therm. Eng. 27 (2007) 145–155, https://doi.org/10.1016/j.applthermaleng.2006.05.007.
[20] J. Shen, Z. Xing, K. Zhang, Z. He, X. Wang, Development of a water-injected twin-screw compressor for mechanical vapor compression desalination systems, Appl. Therm. Eng. 95 (2016) 125–135, https://doi.org/10.1016/j.applthermaleng.2015.11.057.
[21] SKF, Bearing friction, power loss and starting torque. Retrieved from http://www.skf.com/group/products/bearings-units-housings/principles/bearing-selection-process/operating-temperature-and-speed/friction-powerloss-startingtorque/index.html, (n. d.).
[22] N. Stosic, L. Milutinovic, K. Hanjalic, A. Kovavacevic, Investigation of the influence of oil injection upon the screw compressor working process, Int. J. Refrig. 15 (1992) 206–220.
[23] N. Stosic, I.K. Smith, A. Kovacevic, Optimisation of screw compressors, Appl. Therm. Eng. 23 (2003) 1177–1195, https://doi.org/10.1016/S1359-4311(03)00059-0.
[24] Y. Tian, J. Shen, C. Wang, Z. Xing, X. Wang, Modeling and performance study of a water-injected twin-screw water vapor compressor, Int. J. Refrig. (2017), https://doi.org/10.1016/j.ijrefrig.2017.04.008.
[25] Y. Tian, H. Yuan, C. Wang, H. Wu, Z. Xing, Numerical investigation on mass and heat transfer in an ammonia oil-free twin-screw compressor with liquid injection, Int. J. Therm. Sci. 120 (2017) 175–184, https://doi.org/10.1016/j.ijthermalsci.2017.06.007.
[26] D.M. Van de Bor, C.A. Infante Ferreira, A.A. Kiss, Low grade waste heat recovery using heat pumps and power cycles, Energy 89 (2015) 864–873.
[27] D. Zaytsev, Development of wet compressor for application in compression-resorption heat pumps. PhD thesis, Delft University of Technology, 2003.
[28] D. Zaytsev, C.A. Infante Ferreira, Profile generation method for twin screw compressor rotors based on the meshing line, Int. J. Refrig. 28 (2005) 744–755.